Intestinal Fatty Acid-Binding Protein: The Structure and Stability of a Helix-less Variant†

Keehyuk Kim, David P. Cistola,* and Carl Frieden*

Department of Biochemistry and Molecular Biophysics, Washington University School of Medicine, St. Louis, Missouri 63110-1093

Received December 11, 1995; Revised Manuscript Received March 6, 1996⊗

ABSTRACT: The structure of *Escherichia coli*-derived rat intestinal fatty acid-binding protein (I-FABP) exhibits a β-clam topology comprised of two five-stranded antiparallel β-sheets surrounding a large solvent-filled cavity into which the ligand binds. It also contains two α-helices that span residues E15−A32 and join β-strands A and B. This helical domain is conserved in all proteins of this family for which structures have been determined. In order to assess the structural and functional role of the helical domain, we engineered a variant of I-FABP by deleting residues 15−31 and inserting a Ser-Gly linker after residue 14. Circular dichroism measurements indicated that this I-FABP variant, termed Δ17-SG, has a high β-sheet content similar to that of the wild-type protein. Two-dimensional NMR spectra of Δ17-SG revealed patterns similar to those observed for wild-type I-FABP, except for the selective absence of resonances and through-space interactions assigned to the helical domain. The Δ17-SG variant was less stable to denaturant than wild-type I-FABP, but the folding−unfolding transition was highly cooperative and reversible. Taking into account the lower stability, the refolding kinetics of Δ17-SG were essentially identical to those of wild-type. We conclude that Δ17-SG is a helix-less, essentially all-β-sheet variant of I-FABP and that the helical domain is not a required element of the β-clam topology of I-FABP. In addition, the helical domain does not appear to serve as a nucleation site for the refolding process. As shown in the accompanying paper [Cistola, D. P., Kim, K., Rogl, H., & Frieden, C. (1996) *Biochemistry 35*, 7559−7565], the helices may function to regulate the kinetics and energetics of ligand binding.

Intestinal fatty acid-binding protein (I-FABP)[1] belongs to a family of predominately β-sheet proteins that bind a diverse group of polar lipids, such as fatty acids, retinoids, and sterols (Sacchettini & Gordon, 1993; Banaszak *et al*., 1994; Veerkamp & Maatman, 1995). To date, the three-dimensional structures of 11 members of this family have been determined by X-ray crystallography and NMR (Banaszak *et al*., 1994; Haunerland *et al*., 1994; Kleywegt *et al*., 1994; Lassen *et al*., 1995),[2] and all exhibit essentially the same backbone fold. This fold consists primarily of two five-stranded antiparallel β-sheets surrounding a large cavity into which the ligand binds (Figure 1).

Common to these structures is a small helix−turn−helix motif that is interspersed in the sequence between the first and second β-strands. The role of this motif is unknown except that it serves to cover one end of the ligand-binding

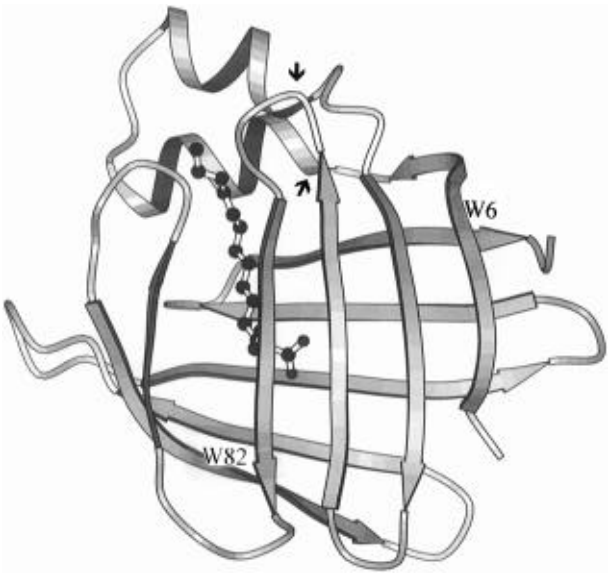

FIGURE 1: Backbone fold of wild-type intestinal fatty acid-binding protein complexed with palmitate. This ribbon diagram is based on the 2.0 Å X-ray crystal structure (Brookhaven file 2ifb; Sacchettini *et al*., 1989) and the NMR chemical shift-derived location of secondary structure elements (Hodsdon *et al*., 1995). To generate the Δ17-SG deletion mutant, amino acids in the α-helical region from residue 15 through 31 (indicated by the arrows) were deleted and replaced by the dipeptide Ser-Gly. The resulting mutant protein appears to be an essentially helix-less, all β-sheet variant of I-FABP. The positions of the two tryptophan residues (W6 and W82) are noted. This diagram was prepared using MOLSCRIPT (Kraulis, 1991).

† This work was supported by National Institutes of Health Grants DK13332 (to C.F.) and DK48046 (to D.P.C.). D.P.C. was supported by a Johnson & Johnson/Merck Research Scholar Award from the American Digestive Health Foundation.

* To whom correspondence should be addressed: Campus Box 8231, Washington University School of Medicine, 660 South Euclid Avenue, St. Louis, MO 63110. Phone: 314-362-3344 or -4382. Fax: 314-362-7183.

⊗ Abstract published in *Advance ACS Abstracts,* May 15, 1996.

[1] Abbreviations: I-FABP, recombinant rat intestinal fatty acid-binding protein; Δ17-SG, a variant of I-FABP engineered by deleting 17 residues (E15−G31) and inserting Ser-Gly after residue Y14; CD, circular dichroism; TOCSY, two-dimensional ^{1}H total correlation spectroscopy; NOESY, two-dimensional ^{1}H nuclear Overhauser and exchange spectroscopy; HSQC, two-dimensional heteronuclear single quantum correlation spectroscopy; Gdn, guanidine hydrochloride.

[2] The NMR solution structure of wild-type I-FABP complexed with palmitate has recently been determined on the basis of 3889 distance constraints derived from three-dimensional ^{13}C- and ^{15}N-resolved NOESY data (M. E. Hodsdon, J. W. Ponder, and D. P. Cistola, manuscript in preparation).

S0006-2960(95)02911-4 CCC: $12.00 © 1996 American Chemical Society

site. The X-ray crystal structure of apo-I-FABP (Scapin *et al*., 1992) does not differ significantly from that of the holoprotein (Sacchettini *et al*., 1992), except for subtle conformational differences involving the helices, the turn between β-strands E and F, and the side chain of F55. These differences have led to the hypothesis that the helical region may be able to form an entry portal for the ligand (Sacchettini *et al*., 1992). However, neither structure reveals an opening large enough to accommodate the entry and exit of the ligand. If the crystal structures are representative of the end states present in solution, then some type of conformational change must occur to allow the entrance of ligand into the internal cavity. Although the mechanism for ligand entry remains unclear, such a conformational change is likely to somehow involve the helical region.

The helical region may also serve an important role in the folding process. As shown elsewhere (Ropson *et al*., 1990), I-FABP can be reversibly unfolded by denaturant. The refolding process appeared to consist of three phases, one of which is too rapid to be observed by stopped-flow techniques. Since helix−coil transitions are very rapid, it seemed possible that the most rapid phase could be related to the helical region of the protein. A related issue is the role that this region might serve in governing the thermodynamic stability of the protein.

For these reasons, we deleted 17 residues comprising the helix−turn−helix domain in an attempt to engineer a helixless, all-β-sheet variant of I-FABP. The deleted region is located between the arrows shown in Figure 1. In order to connect the newly created N- and C-terminal ends, a Ser-Gly dipeptide linker was inserted after residue 14. As shown below, this I-FABP variant (Δ17-SG) does not exhibit any α-helical characteristics and the overall β-sheet conformation is preserved. While this sequence deletion does lower the midpoint of guanidine denaturation and significantly destabilizes the protein, the refolding kinetics are very similar to those of the wild-type protein. In addition, the protein retains its ability to bind fatty acids with some features resembling those of the wild-type protein, as addressed in the accompanying paper (Cistola *et al*., 1996).

MATERIALS AND METHODS

Materials. A mutagenic primer was obtained from Integrated DNA Technologies. The Sculptor *in vitro* site-directed mutagenesis kit and [α-^{35}S]ATP were purchased from Amersham. The Sequenase v2.0 sequencing kit was from United States Biochemical. Oleic acid (Sigma Chemical) was dissolved in 0.1 M potassium hydroxide to make a 5 mM stock solution. Ultrapure Gdn was obtained from ICN Biochemicals. All other reagents used were analytical grade.

Protein Engineering and Expression. Site-directed mutagenesis was used to delete 17 residues, with a mutagenic oligomer lacking the amino acid codons from Glu15 through Gly31. The codons for two amino acids, Ser and Gly, were inserted in their place to provide a link between Tyr14 and Ala32. The sequence of the mutagenic oligomer was 5′-TTTCAAGTTGTCATGAGCACCACTATAGT-TCTCATTCCGGTC-3′. The deletion and insertion were confirmed by complete sequencing of the entire cDNA encoding the variant I-FABP. The mutant protein was overexpressed in *Escherichia coli* harboring the pMON-IFABP plasmid and purified using the published protocol for wild-type I-FABP (Sacchettini *et al.*, 1990) with minor modifications. The mutant protein was overexpressed from a *rec*A promoter by adding 0.1 mM nalidixic acid. The cell paste was homogenized using a French press and was stirred at 4 °C while 80% ammonium sulfate solution was added until the final concentration reached 50%. The soluble fraction of cell lysate in 50% ammonium sulfate was applied to a phenyl sepharose CL-4B (Pharmacia) column pre-equilibrated with 2 M ammonium sulfate in 20 mM Tris-HCl (pH 8.0) and 0.25 mM EDTA and eluted with 20 mM Tris-HCl (pH 8.0) and 0.25 mM EDTA. Fractions containing the mutant protein were pooled and diluted until an ionic strength lower than 2.1 mmho was obtained. The protein was bound to Zeta-prep QAE and was eluted by a 0 to 0.2 M KCl gradient. The pooled fraction was concentrated in an Amicon ultrafiltration unit using a YM-10 membrane. The protein was delipidated as described previously (Glatz & Veerkamp, 1983). The mutant protein appeared as a single band on SDS−PAGE gels and migrated with the expected lower molecular mass (13.3 kDa) compared with that of the wild-type protein (15.1 kDa). The mutant protein was stable, and no aggregation was observed during purification and storage at 4 °C.

Uniformly ^{13}C/^{15}N-enriched I-FABP (Δ17-SG) was biosynthesized and purified using protocols detailed elsewhere (Hodsdon *et al*., 1995). The final yield of purified, delipidated, isotope-enriched protein was approximately 95 mg. A portion of this protein was complexed with a stoichiometric amount of perdeuterated palmitic acid, as described by Cistola *et al.* (1989).

Circular Dichroism. Spectra were collected using a Jasco J600 spectropolarimeter. The path length of the cell was 0.1 cm, and the protein concentration was adjusted to 0.11 and 0.12 mg/mL for wild-type I-FABP and Δ17-SG, respectively. All measurements were made in 10 mM potassium phosphate buffer at pH 7.4 and ambient temperature.

NMR Spectroscopy. All spectra were accumulated using a three-channel Varian Unity-500 NMR spectrometer equipped with a Nalorac 5 mm IDTG 500-5 gradient inverse triple-resonance probe and interfaced to a Sun SPARC-2 workstation. The buffer used for NMR was 20 mM potassium phosphate, 50 mM potassium chloride, and 0.05% sodium azide (pH 7.2), and all spectra were accumulated at 25 °C unless noted otherwise. Two-dimensional TOCSY spectra (Bax & Davis, 1985) were collected using an unenriched protein sample containing an 80% H_2O-based buffer and a MLEV-17 mixing time of 20 ms. Two-dimensional NOESY spectra (Jeener *et al*., 1979) were collected using unenriched protein samples containing either an 80% H_2O- or "100%" D_2O-based buffer and a mixing time of 150 ms. The pulse sequence used for the gradient- and sensitivity-enhanced ^{1}H/^{15}N HSQC experiments was that of Zhang *et al.* (1994). For these experiments, a uniformly ^{13}C/^{15}N-enriched protein sample containing an 80% H_2O-based buffer was used. Proton and nitrogen chemical shifts were referenced as described by Hodsdon *et al*. (1995).

Determination of Stability in Gdn. Equilibrium unfolding and refolding as a function of denaturant concentration in 20 mM potassium phosphate (pH 7.4) and 0.25 mM EDTA was monitored by fluorescence spectroscopy with excitation at 290 nm and emission at 328 nm on a PTI Alphascan fluorometer (Photon Technology International). Both wild-

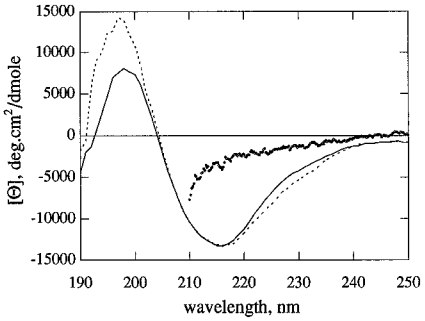

FIGURE 2: CD spectra of the wild-type (- - -) and Δ17-SG (—) forms of I-FABP in 10 mM potassium phosphate, at pH 7.4 and ambient temperature. Also shown is the spectrum of 2 M Gdn-denatured Δ17-SG I-FABP (●). The concentrations were 0.11 and 0.12 mg/mL for the wild-type and mutant proteins, respectively.

type and mutant proteins incubated overnight in 2 M Gdn showed no further changes in fluorescence and were then used in folding experiments. Equilibrium data were fit to a two-state model as described by Ropson *et al.* (1990) with an equation from Santoro and Bolen (1988).

Refolding Kinetics. The kinetics of refolding were followed by fluorescence using an Applied Photophysics stopped-flow spectrophotometer (Model SFMV12) interfaced to an Archimedes 420 (Acorn) computer. Changes in fluorescence ($\lambda_{excitation} = 290$ nm and $\lambda_{emission} > 305$ nm with a WG305 Schott glass filter) were followed at 20 °C. The unfolded proteins were preincubated in 2.0 M (wild-type) or 1.2 M (Δ17-SG) Gdn buffered in 20 mM potassium phosphate (pH 7.4) and 0.25 mm EDTA and were diluted 2-fold by mixing with an equal volume of buffer. The fluorescence of the native protein in buffer solution and in Gdn were measured at the same time and used as reference points. Although the high concentration of Gdn resulted in a mixing artifact on dilution, optical turbulence appeared to last less than 40 ms.

RESULTS

In this study, 17 residues from E15 to G31 have been deleted from the sequence of I-FABP and replaced with the dipeptide Ser-Gly. We hypothesized that this alteration of the I-FABP sequence might generate a stable, all-β-sheet structure lacking the two helices. The experiments described in this paper were designed to test this hypothesis and to make an initial assessment of the structure and stability of this I-FABP variant.

Conformation of Δ17-*SG as Assessed by Circular Dichroism and Fluorescence Spectroscopy.* Initial studies of the structure of Δ17-SG involved CD measurements in the far-UV. Figure 2 shows CD spectra for wild-type and Δ17-SG as well as for the latter protein in the presence of denaturant. While CD spectra of highly β-sheet structures are difficult to analyze, it is clear that the spectra for the wild-type and variant proteins are very similar and that both are quite different from unfolded protein (Figure 2). Thus, Δ17-SG appears to have at least as much β-sheet content as the wild-type protein, and the smaller signal at 196 nm is consistent with loss of α-helical content (Brahms *et al.*, 1980). Similarly, fluorescence spectra not shown here indicated that the emission maximum, with excitation at 290 nm, was the same for the folded wild-type and Δ17-SG proteins ($E_{max} =$ 328 nm), although the fluorescence intensity of Δ17-SG was about 20% greater than that for wild-type I-FABP. For both proteins, the fluorescence maximum decreased and shifted to 350 nm in the presence of denaturant.

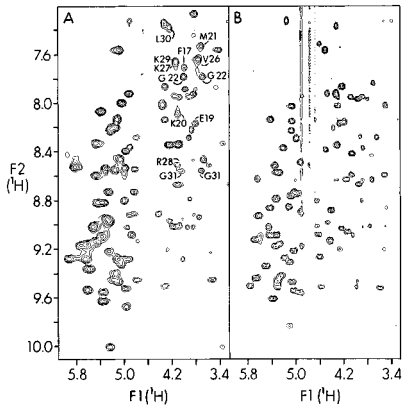

FIGURE 3: Fingerprint region of 2D TOCSY spectra for the wild-type (A) and Δ17-SG (B) I-FABP complexed with palmitate in an 80% H_2O/20% D_2O-based buffer. The protein concentration was 2 mM. Both spectra utilized a spin lock mixing time of 20 ms. Aquisition and processing parameters for spectrum A were as follows: 96 transients, 512 t_1 increments zero-filled to 1024, 6500 Hz spectral width in F1 and F2, and 1024 complex points in t_2 zero-filled to 2048. Aquisition and processing parameters for spectrum B were as follows: 64 transients, 256 t_1 increments zero-filled to 1024, 6000 Hz spectral width in F1 and F2, and 1024 complex points in t_2 zero-filled to 2048. For both proteins, pseudo-echo apodization was employed in both dimensions. The sample temperature for spectrum A was 37 °C, chosen to match the conditions used for the assignment of the wild-type protein (Hodsdon *et al.*, 1995). To minimize protein aggregation, a temperature of 25 °C was used for Δ17-SG in spectrum B. The chemical shifts for the wild-type protein at 25 °C differ only slightly from those at 37 °C.

Conformation of Δ17-*SG as Assessed by NMR Spectroscopy.* Two-dimensional TOCSY, NOESY, and $^1H/^{15}N$ HSQC spectra were recorded and compared to those of wild-type I-FABP in order to further characterize the secondary and tertiary structures of Δ17-SG. Sequence-specific ^1H, ^{13}C, and ^{15}N NMR resonance assignments and solution structures have been established for the wild-type protein (Hodsdon *et al.*, 1995),[2] thus providing a basis for the comparison of chemical shifts and NOE patterns.

The chemical shifts of $^1H\alpha$ resonances in proteins are affected by backbone conformation (Wishart *et al.*, 1991, 1992), and ^1H and ^{13}C chemical shift indices have been used to map the secondary structure elements of wild-type I-FABP (Hodsdon *et al.*, 1995). In addition, the chemical shifts of ^1HN resonances are influenced by backbone conformation as well as by hydrogen bond energies (Wishart *et al.*, 1991). Therefore, the fingerprint region of the TOCSY spectrum, which correlates intraresidue $^1H\alpha$ and ^1HN chemical shifts, is quite sensitive to changes in secondary and tertiary structure.

The fingerprint regions of TOCSY spectra for wild-type and Δ17-SG I-FABP are shown in Figure 3. Overall, both spectra revealed a high degree of chemical shift dispersion, indicative of highly structured proteins. While the cross-peaks in Figure 3A,B were not superimposable, similar overall patterns were observed. Chemical shift values are very sensitive to changes in local environment as well as global structure, so chemical shift changes would be expected to occur upon deletion of a 17-residue segment of the protein. However, these differences are relatively small and still consistent with a similar structure for the β-sheet domain

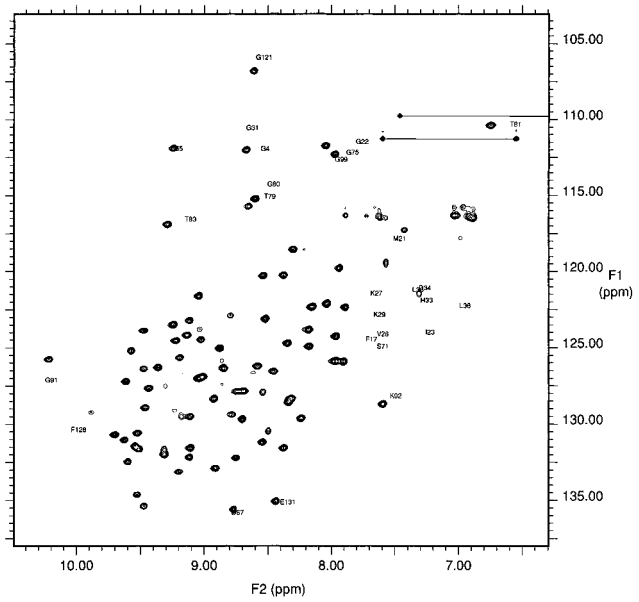

FIGURE 4: Gradient- and sensitivity-enhanced $^1H/^{15}N$ HSQC spectrum for [U-88%-^{13}C/99%-^{15}N]I-FABP (Δ17-SG) complexed with palmitate at 25 °C. Superimposed on the spectrum of the mutant protein are labels indicating the positions of assigned resonances for the wild-type protein. For clarity, labels were included only at the periphery of the spectrum. The complete HSQC map for wild-type protein is shown in Figure 1 of Hodsdon *et al*. (1995). Aquisition parameters were as follows: 24 transients; 600 t_1 increments; spectral widths of 6500 Hz (F2) and 3000 Hz (F1); hypercomplex mode; pulse interval, 1.1 s; and sample concentration, 1.7 mM.

(see below). In particular, note that the region corresponding to $^1H\alpha \geq 4.2$ ppm was well-populated with cross-peaks. In the wild-type protein, all of the $^1H\alpha$ peaks ≥ 4.2 ppm are located in β-strands or turns (Hodsdon *et al*., 1995). In contrast, many of the cross-peaks corresponding to the α-helical domain of the wild-type protein (labeled in the upper right of Figure 3A) are absent in Δ17-SG (Figure 3B).

Figure 4 illustrates a $^1H/^{15}N$ HSQC spectrum for uniformly $^{13}C/^{15}N$-enriched I-FABP (Δ17-SG). Superimposed on this spectrum are labels indicating the positions of a number of peaks for the *wild-type* protein. The completely assigned wild-type spectrum is shown elsewhere (Hodsdon *et al*., 1995), and the assignment of Δ17-SG is in progress. For now, the spectra can be compared. Both spectra exhibit a high degree of chemical shift dispersion and a similar overall $^1H/^{15}N$ correlation map. In fact, a number of resonances from the β-sheet domain of the protein are nearly superimposable; examples include D67 and E131 at the bottom of Figure 4 and G65 and G121 near the top. In contrast, many of the peaks assigned to the α-helix domain of the wild-type protein are absent in the Δ17-SG spectrum. Notable examples include F17, G22, I23, V26, K27, K29, and G31.

The average chemical shifts for both proteins are summarized in Table 1. For wild-type I-FABP, the $^1H\alpha$, ^1HN, and ^{15}N chemical were lower for residues located in α-helices than in with β-sheets and turns. In the absence of sequential assignments for Δ17-SG, the chemical shift values cannot yet be partitioned and compared in this way. However, the average values for all residues could be compared for the wild-type and Δ17-SG proteins. As seen in Table 1, the average values of $^1H\alpha$ and ^{15}N chemical shifts for Δ17-SG each exhibited statistically significant increases compared with those of the wild-type protein. These increases are consistent with a reduction in α-helix content for Δ17-SG.

Table 1: Average Chemical Shift Values for Wild-Type and Δ17-SG I-FABP

resonance type[a]	I-FABP (wild-type)[b] (ppm)	I-FABP (Δ17-SG)[b] (ppm)
$^1H\alpha$, all residues	4.57 ± 0.65	4.80 ± 0.60[c]
$^1H\alpha$, helix only	3.88 ± 0.23	
$^1H\alpha$, nonhelix	4.69 ± 0.58	
^1HN, all residues	8.54 ± 0.69	8.70 ± 0.68[d]
^1HN, helix only	7.90 ± 0.48	
^1HN, nonhelix	8.62 ± 0.66	
^{15}N, all residues	123.5 ± 13.0	125.6 ± 6.0[c]
^{15}N, helix only	120.7 ± 4.6	
^{15}N, nonhelix	123.8 ± 13.7	

[a] All ^1HN and ^{15}N chemical shifts represent backbone positions. [b] Values reported as mean ± standard deviation. [c] Statistically significant difference ($p < 0.05$) *vs* wild-type; independent-samples *t* test. [d] No statistically significant difference ($p > 0.05$) *vs* wild-type.

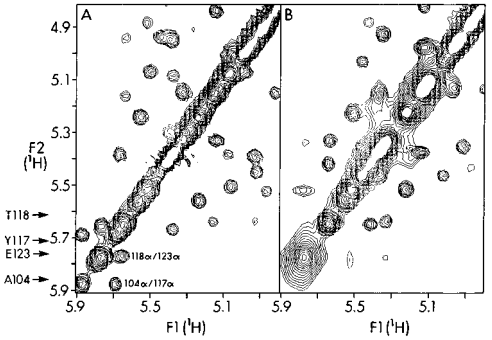

FIGURE 5: αα region of 2D NOESY spectra of wild-type (A) and Δ17-SG (B) I-FABP complexed with palmitate at 25 °C. Intense cross-peaks in this region are characterisitic of β-sheet-containing proteins. The labels indicate the positions of assigned resonance and correlations for the wild-type protein at 37 °C (Hodsdon *et al*., 1995). Both samples contained 100% D_2O-based buffer and protein concentrations of 2 mM. Aquisition and processing parameters were as follows: 96 transients, 256 t_1 increments zero-filled to 1024, 6500 Hz spectral width in F1 and F2, 1024 complex points in t_2 zero-filled to 2048, and 150 ms mixing time.

Two-dimensional NOESY spectra were accumulated on the unenriched proteins in order to search for patterns characteristic of α-helix and β-sheet secondary structure. Regions of a protein containing antiparallel β-sheets exhibit NOESY cross-peaks corresponding to short interstrand αα and sequential αN interproton distances (Wüthrich, 1986). Portions of the αα region of NOESY spectra for wild-type and Δ17-SG I-FABP are shown in panels A and B of Figure 5, respectively. The spectra for both proteins exhibited a number of intense αα (Figure 5) and αN (not shown) correlations indicative of β-sheet structure. However, only the spectrum of Δ17-SG showed a selective broadening for the αα peaks between 5.6 and 5.9 ppm. In the wild-type protein, these cross-peaks represent correlations between the α-protons of T118 (end of β-strand I) and E123 (beginning of β-strand J), as well as between A104 (beginning of β-strand H) and Y117 (end of β-strand I). Strands H−J are the carboxy terminal β-strands located at the "back" of the molecule as oriented in Figure 1. The above-mentioned residues are adjacent to the helices, and the selective deletion of the helices might be expected to destablize this portion of the protein. Hence, the peak broadening/conformational averaging observed in Figure 5B is consistent with the selective elimination of the helical domain of I-FABP.

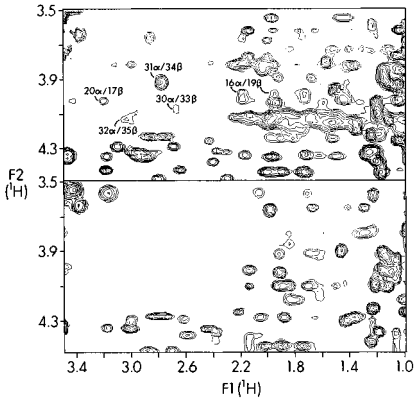

FIGURE 6: $\alpha\beta$ region of 2D NOESY spectra of wild-type (upper panel) and Δ17-SG (lower panel) I-FABP complexed with palmitate at 25 °C. The labels indicate correlations between residues *i* and *i*+3 in the α-helical region of the wild-type protein. Note the absense of these correlations in Δ17-SG. The sample and spectral conditions were as in Figure 5.

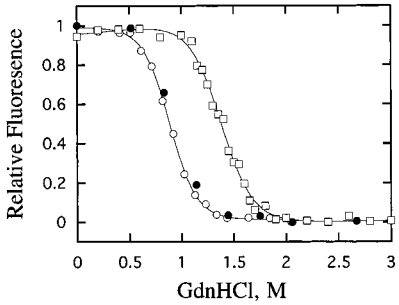

FIGURE 7: Equilibrium unfolding of apo-wild-type (□) and Δ17-SG (○) I-FABP. Changes in relative fluorescence ($\lambda_{excitation}$ = 290 nm, $\lambda_{emission}$ = 328 nm) were monitored as a function of Gdn concentration at 20 °C. The open symbols represent the dilution of the protein to a buffer containing final concentrations of denaturant shown. The closed symbols show the reversibility of the transition, where the Δ17-SG protein was equilibrated in 2.7 M Gdn and then diluted to the final concentrations of denaturant as shown. The same dilution of the native helix-less protein was used as a reference at 0 M Gdn. All solutions contained 20 mM potassium phosphate (pH 7.4) and 0.25 mM EDTA.

A region of the NOESY spectrum containing $\alpha\beta$ correlations is shown in Figure 6. Helices are characterized by short $\alpha\beta$ interproton distances between the *i* and *i*+3 residues (Wüthrich, 1986). In the upper panel of Figure 6, the labeled cross-peaks indicate several such correlations for the wild-type protein. By contrast, these correlations were absent in the spectrum of Δ17-SG (Figure 6, lower panel).

Protein Stability as Assessed by Equilibrium Studies of Denaturation and Renaturation. Since the fluorescence spectrum is affected by denaturant, it is possible to use fluorescence to describe the equilibrium unfolding and refolding of the protein. Figure 7 shows an equilibrium unfolding/refolding curve as a function of Gdn concentration. The open symbols represent the unfolding process, while the filled circles are data obtained upon refolding the protein. The figure shows that the unfolding is reversible but that Δ17-SG is less stable than wild-type I-FABP. Table 2 presents the analysis of these data. As an indication of stability, the midpoint of the denaturation curve for the apo-wild-type protein is 1.36 M Gdn (Ropson *et al.*, 1990) and that for Δ17-SG is 0.89 M Gdn.

Kinetics of Refolding. We have previously shown that the refolding process of I-FABP occurs in three phases, one of which is too rapid to measure by stopped-flow techniques

Table 2: Stability of Wild-Type and Δ17-SG I-FABP[a]

I-FABP	ΔG_{H_2O}[b] (kcal mol^{-1})	m_G[c] (kcal mol^{-1} M^{-1})	midpoint[d] (M)
wild-type	5.22 ± 0.33	−3.82 ± 0.21	1.36 ± 0.11
Δ17-SG	4.04 ± 0.15	−4.56 ± 0.17	0.89 ± 0.05

[a] All solutions contained 20 mM potassium phosphate (pH 7.4) and 0.25 mM EDTA. Relative fluorescence changes at 328 nm (λ_{ex} = 290 nm) were monitored as a function of Gdn concentrations at 20 °C. [b] The apparent free energy difference between the folded and unfolded forms of I-FABP extrapolated to 0 M denaturant. [c] The slope describing the dependence of Δ*G* on denaturant concentrations. [d] The denaturant concentration at the midpoint of the transition.

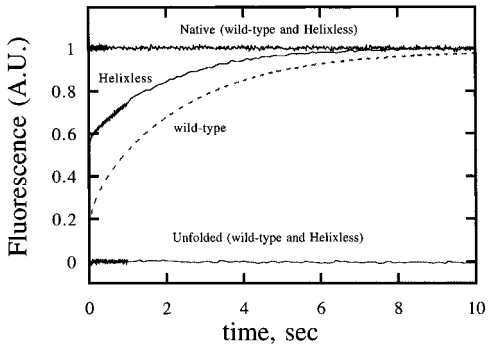

FIGURE 8: Changes in fluorescence intensity (arbitrary units) *vs* time for the refolding of wild-type and Δ17-SG I-FABP. The experiments were performed as described in Materials and Methods. For the unfolded base line, protein was mixed with an equal volume of either 2 M Gdn for wild-type or 1.2 M Gdn for the Δ17-SG I-FABP under the same experimental conditions. Equal volumes of native protein and buffer were mixed and used to establish the base line for the native proteins. The base line values have been normalized to 0 (unfolded protein) and 1 (native protein) for both the wild-type and helix-less proteins.

(Ropson *et al.*, 1990). As expected for a protein that contains no proline, the rate constants for the refolding process increase as the final denaturation concentration is lowered. Additionally, the extent of the very rapid phase is also dependent on the final denaturant concentration (Ropson *et al.*, 1990). However, both of these parameters, rate constants and extents, depend not on the absolute final concentration of denaturant but on the final concentration relative to the midpoint of the unfolding/refolding curve. Thus, to compare refolding kinetics between wild-type and Δ17-SG, it is necessary to choose final denaturant concentrations which are related to the unfolding midpoint. Figure 8 shows the fluorescence changes occurring on a 2-fold dilution of denaturant. For wild-type, the dilution was from 2 to 1 M Gdn (midpoint = 1.39 M). For Δ17-SG, the dilution was from 1.2 to 0.6 M Gdn (midpoint = 0.89 M). Also shown in the figure are base line fluorescence values for completely unfolded and folded (native) protein. Both proteins exhibited a very rapid phase followed by a slower phase with folding completed in 10 s under these conditions. The very rapid phase had a larger amplitude for Δ17-SG as compared with wild-type, although the observed rate constants were similar. For the wild-type I-FABP, the observed rate constant was 0.43 s^{-1}, while for Δ17-SG, it was 0.51 s^{-1}. Thus, the α-helical domain appeared to have little influence on the refolding kinetics of I-FABP.

DISCUSSION

A variant of I-FABP has been engineered by deleting 17 residues corresponding to the α-helical domain and inserting

a two-residue linker. This variant has been characterized by CD, fluorescence, and NMR spectroscopy and compared with the wild-type protein in order to assess its solution conformation, thermodynamic stability, and folding properties.

Δ17-SG Is a Helix-less Variant of I-FABP. Several lines of evidence support the hypothesis that Δ17-SG is a helix-less, essentially all-β-sheet variant of I-FABP. First, the CD and fluorescence spectra for this variant were very similar to those for wild-type I-FABP. The CD spectrum of the wild-type protein was largely dominated by the high β-sheet content of the protein, and that of Δ17-SG was even more like a β-sheet protein. Second, two-dimensional NMR spectra of Δ17-SG exhibited a high degree of chemical shift dispersion and overall patterns similar to those of the wild-type protein. A number of the $^{1}H/^{15}N$ HSQC resonances for Δ17-SG were nearly superimposable with those of the wild-type protein. Third, the TOCSY, NOESY, and HSQC spectra of Δ17-SG revealed a selective absence of resonances assigned to the helical region of the wild-type protein. The NOESY spectra showed a number of αα and αN correlations consistent with a high β-sheet content. Finally, the average chemical shift values for the $^{1}H\alpha$, ^{1}HN, and ^{15}N positions were consistent with a β-sheet structure with considerably less α-helical content than the wild-type protein. Although a more detailed characterization of the structure of Δ17-SG must await further studies using multidimensional NMR and X-ray crystallography, the above evidence collectively argues for a structural model similar to that shown in Figure 1 except for the lack of the helix−turn−helix region.

Possible Roles for the Helical Domain in I-FABP and Other Lipid-Binding Proteins. The high degree of topological conservation of the helical domain in the intracellular lipid-binding protein family implies that it serves an important structural and/or functional role. However, this role has remained undefined. Several possibilities are that the helical domain (1) stabilizes the overall β-clam topology of the protein, (2) serves as a nucleation site for protein folding, (3) governs the nature of ligand binding, including the mechanism of entry and exit, and/or (4) mediates protein−protein and protein−membrane interactions important in the intracellular function of the protein.

The Δ17-SG I-FABP employed in this study provides a unique model system for addressing the above questions. From the present results, it is clear that the helical domain is not a required element of the overall-β-clam topology of I-FABP. Although Δ17-SG is less stable than wild-type protein, it is still able to fold into an essentially all β-sheet protein. In the wild-type protein, the amino groups of Lys20 and Lys27 of the helical region are hydrogen bonded to the carboxyl groups of Glu120 and Asp74, respectively. The loss of hydrogen bonds between residues in the α-helical and β-sheet domains of the protein presumably contributes to the lower stability of Δ17-SG. Also, a number of van der Waals contacts are also lost and the solvent accessible surface of the protein appears to be more hydrophobic with the removal of the relatively polar helical domain.

The α-helical domain apparently does not serve as a nucleation site for protein folding. The kinetics of refolding, taking into account the difference in stability, were unaffected by the lack of the α-helices. Thus, the α-helical domain does not appear to play a significant role in the refolding process. This conclusion is consistent with previous ^{19}F NMR studies which indicated that a hydrophobic region near Trp82, located at the opposite end of I-FABP, may be involved in a structural intermediate that forms early in the folding process (Ropson & Frieden, 1992; Frieden *et al*., 1993, 1995).

The role of the α-helical domain in ligand binding is addressed in the accompanying paper (Cistola *et al.*, 1996). This domain appears to regulate the affinity of fatty acid binding by selectively altering the dissociation rate constant.

ACKNOWLEDGMENT

The authors thank Dr. Lewis E. Kay (University of Toronto) for providing the source code for the gradient- and sensitivity-enhanced $^{1}H/^{15}N$ HSQC experiment and Dr. James J. Toner for the biosynthesis and purification of $^{13}C/^{15}N$-enriched Δ17-SG.

REFERENCES

Banaszak, L. B., Winter, N., Xu, Z., Bernlohr, D. A., Cowan, S., & Jones, T. A. (1994) *Adv. Protein Chem. 45*, 89−151.

Bax, A., & Davis, D. G. (1985) *J. Magn. Reson. 65*, 355−360.

Brahms, S., & Brahms, J. (1980) *J. Mol. Biol. 138*, 149−178.

Cistola, D. P., Sacchettini, J. C., Banaszak, L. J., Walsh, M. T., & Gordon, J. I. (1989) *J. Biol. Chem. 264*, 2700−2710.

Cistola, D. P., Kim, K., Rogl, H., & Frieden, C. (1996) *Biochemistry 35*, 7559−7565.

Frieden, C., Hoeltzli, S. D., & Ropson, I. J. (1993) *Protein Sci. 2*, 2007−2014.

Frieden, C., Jiang, N., & Cistola, D. P. (1995) *Biochemistry 34*, 2007−2014.

Glatz, J. F. C., & Veerkamp, J. H. (1983) *Anal. Biochem. 132*, 89−95.

Haunerland, N. H., Jacobson, B. L., Wesenberg, G., Rayment, I., & Holden, H. M. (1994) *Biochemistry 33*, 12378−12385.

Hodsdon, M. E., Toner, J. J., & Cistola, D. P. (1995) *J. Biomol. NMR 6*, 198−210.

Jeener, J., Meier, B. H., Bachmann, P., & Ernst, R. R. (1979) *J. Chem. Phys. 71*, 4546−4552.

Kleywegt, G. J., Bergfors, T., Senn, H., Le Motte, P., Gsell, B., Shudo, K., & Jones, T. A. (1994) *Structure 2*, 1241−1258.

Kraulis, P. (1991) *J. Appl. Crystallogr. 24*, 946−950.

Lassen, D., Lücke, C., Kveder, M., Mesgarzadeh, A., Schmidt, J. M., Specht, B., Lezius, A., Spener, F., & Rüterjans, H. (1995) *Eur. J. Biochem. 230*, 266−280.

Ropson, I. J., & Frieden, C. (1992) *Proc. Natl. Acad. Sci. U.S.A. 89*, 7222−7226.

Ropson, I. J., Gordon, J. I., & Frieden, C. (1990) *Biochemistry 29*, 9591−9599.

Sacchettini, J. C., & Gordon, J. I. (1993) *J. Biol. Chem. 268*, 18399−18402.

Sacchettini, J. C., Gordon, J. I., & Banaszak, L. J. (1989) *J. Mol. Biol. 208*, 327−339.

Sacchettini, J. C., Banaszak, L. J., & Gordon, J. I. (1990) *Mol. Cell. Biochem. 98*, 81−93.

Sacchettini, J. C., Scapin, G., Gopaul, D., & Gordon, J. I. (1992) *J. Biol. Chem. 267*, 23534−23545.

Santoro, M. M., & Bolen, D. W. (1988) *Biochemistry 27*, 8063−8068.

Scapin, G., Gordon, J. I., & Sacchettini, J. C. (1992) *J. Biol. Chem. 267*, 4253−4269.

Veerkamp, J. H., & Maatman, R. G. H. J. (1995) *Prog. Lipid Res. 34*, 17−52.

Wishart, D. S., Sykes, B. D., & Richards, F. M. (1991) *J. Mol. Biol. 222*, 311−333.

Wishart, D. S., Sykes, B. D., & Richards, F. M. (1992) *Biochemistry 31*, 1647−1651.

Wüthrich, K. (1986) *NMR of Proteins and Nucleic Acids*, pp 162−166, John Wiley & Sons, New York.

Zhang, O., Kay, L. E., Olivier, J. P., & Forman-Kay, J. D. (1994) *J. Biomol. NMR 4*, 845−858.

BI9529115